Removing deep brain stimulation artifacts from the electroencephalogram: Issues, recommendations and an open-source toolbox

Article *in* Clinical Neurophysiology · August 2018

DOI: 10.1016/j.clinph.2018.07.023

CITATIONS
2

READS
388

5 authors, including:

Guillaume Lio
French National Centre for Scientific Research
21 PUBLICATIONS **107** CITATIONS
SEE PROFILE

Bénédicte Ballanger
French National Centre for Scientific Research
54 PUBLICATIONS **1,720** CITATIONS
SEE PROFILE

Brian Lau
L'Institut du Cerveau et de la Moelle Épinière
53 PUBLICATIONS **1,667** CITATIONS
SEE PROFILE

Philippe Boulinguez
Claude Bernard University Lyon 1
49 PUBLICATIONS **1,236** CITATIONS
SEE PROFILE

Clinical Neurophysiology 129 (2018) 2170–2185

Contents lists available at ScienceDirect

Clinical Neurophysiology

journal homepage: www.elsevier.com/locate/clinph

Removing deep brain stimulation artifacts from the electroencephalogram: Issues, recommendations and an open-source toolbox

Guillaume Lio [a,b,c], Stéphane Thobois [a,b,c,d], Bénédicte Ballanger [a,b,e], Brian Lau [f], Philippe Boulinguez [a,b,e,*]

[a] Université de Lyon, F-69622 Lyon, France
[b] Université Lyon 1, Villeurbanne, France
[c] CNRS, Centre de Neuroscience Cognitive, Bron, France
[d] Hospices civils de Lyon, hôpital neurologique Pierre Wertheimer, Bron, France
[e] INSERM U1028, CNRS UMR5292, Centre de Recherche en Neurosciences de Lyon, Lyon, France
[f] Sorbonne Universités, UPMC Univ Paris 06, UMR S 1127, CNRS UMR 7225, Institut du Cerveau et de la Moelle épinière, F-75013 Paris, France

ARTICLE INFO

Article history:
Accepted 28 July 2018
Available online 13 August 2018

Keywords:
Deep brain stimulation
EEG
MEG
Artifacts
Antialiasing
Oversampling
Low-pass filtering
Matched filters
Hampel
Template subtraction
ICA

HIGHLIGHTS

- Antialiasing analog filters are not designed to protect against DBS artifacts in EEG.
- Low-pass temporal filtering is insufficient: DBS also causes low-frequency artifacts.
- Tracking outliers in the frequency domain is necessary to remove DBS artifacts.

ABSTRACT

A major question for deep brain stimulation (DBS) research is understanding how DBS of one target area modulates activity in different parts of the brain. EEG gives privileged access to brain dynamics, but its use with implanted patients is limited since DBS adds significant high-amplitude electrical artifacts that can completely obscure neural activity measured using EEG. Here, we systematically review and discuss the methods available for removing DBS artifacts. These include simple techniques such as oversampling, antialiasing analog filtering and digital low-pass filtering, which are necessary but typically not sufficient to fully remove DBS artifacts when each is used in isolation. We also cover more advanced methods, including techniques tracking outliers in the frequency-domain, which can be effective, but are rarely used. The reason for that is twofold: First, it requires advanced skills in signal processing since no user friendly tool for removing DBS artifacts is currently available. Second, it involves fine-tuning to avoid over-aggressive filtering. We highlight an open-source toolbox incorporating most artifact removal methods, allowing users to combine different strategies.

Contents

* Corresponding author at: CRNL, bâtiment IDEE, 59 Boulevard Pinel, 69500 Bron, France.
E-mail address: philippe.boulinguez@univ-lyon1.fr (P. Boulinguez).

https://doi.org/10.1016/j.clinph.2018.07.023
1388-2457/

1. Introduction

During the past two decades, deep brain stimulation (DBS) has been recognized as an efficient therapy that alleviates the symptoms of various treatment-resistant movement disorders such as Parkinson's disease (PD), dystonia, and tremor (Lyons, 2011; Vidailhet et al., 2013; Aviles-Olmos et al., 2014; Fasano et al., 2014; Kalia et al., 2013; Larson, 2014). Recent reports suggest that DBS can also be effective for treating psychiatric disorders such as depression, obsessive-compulsive disorder, Tourette's syndrome (Holtzheimer and Mayberg, 2011) as well as dementia-related disorders and Alzheimer's disease (Laxton et al., 2013; Hescham et al., 2013). However, the mechanisms underlying the therapeutic success of DBS remain somewhat mysterious (Dostrovsky and Lozano, 2002; McIntyre et al., 2004; Kringelbach et al., 2007; Bourne et al., 2012). While initially conceived as a "reversible lesion", it is increasingly clear that DBS may produce a more complex neurophysiological response (Vitek, 2008; Agnesi et al., 2013; Chiken and Nambu, 2014), not only within but also outside the local circuits targeted by the stimulation. Indeed, the best sites of implantation of the DBS electrodes correspond to regions where the effects of stimulation may be widespread due to activation of multiple pathways (Hammond et al., 2008; Ponce and Lozano, 2010). This is especially the case of the thalamus and subthalamic nucleus (STN), which are at the core of the cortical-thalamic-basal ganglia-cortical network.

Therefore, it is a major issue to understand how DBS of one target area modulates activity in different parts of the brain (Okun, 2014). First, gaining access to the mechanisms of action of DBS may provide important information regarding clinical practice, in particular how some symptoms are alleviated, and how side effects might occur. Second, DBS and associated pathologies also represent important models for studying the neural bases of numerous psychological functions. So far, functional imaging with positron emission tomography (PET) has provided a unique window for analyzing *in vivo* the consequences of DBS on whole brain activation patterns (e.g., Ballanger et al., 2009a; Ko et al., 2013). Indeed, although possible (e.g., Jech et al., 2001, 2012; Phillips et al., 2006; Holiga et al., 2015), the use of functional magnetic resonance imaging (fMRI) is limited with implanted patients for safety reasons (Rezai et al., 2004; Carmichael et al., 2007). As a consequence, direct assessment remains challenging because PET does not allow event-related analysis of brain activations (e.g., Ballanger et al., 2009b).

Electrophysiological recordings might thus appear as an ideal solution to track brain dynamics under DBS. While local field potential recordings made from the targeted areas of patients undergoing DBS have added greatly to the understanding of the local effects of stimulation (Rosa et al., 2012; Lempka and McIntyre, 2013; Little et al., 2013; Thompson et al., 2014; de Hemptinne et al., 2015), they cannot inform about whole brain dynamics. Electroencephalography (EEG) does. Advanced EEG signal processing methods now allow efficient source separation and localization (e.g., Huster and Calhoun, 2018; Huster and Raud, 2018; Lio and Boulinguez, 2013, 2018; Makeig et al., 2004; Michel and Murray, 2012; Michel et al., 2004; Michel and He, 2011; Pascual-Marqui, 2009; Tang et al., 2005), which permits using EEG to study the effects of DBS on whole brain activity. However, despite increasing interest (Fig. 1), there are still relatively few studies that have analyzed brain activity with EEG during DBS. There are several possible reasons for not using EEG to analyze and localize DBS-induced brain activity modulations. The first one is that it requires sophisticated data analysis to extract useful spatial information from the EEG (Makeig and Onton, 2009). This first limitation can easily be circumvented. Today, several interactive graphic user interfaces (GUIs) offer a wealth of solutions for performing advanced processing of EEG data (e.g., Delorme and Makeig, 2004; Dalal et al., 2004; Delorme et al., 2011; Tadel et al., 2011; Oostenveld et al., 2011). As such, modeling event-related brain dynamics with good spatial and optimal temporal resolutions by means of EEG recordings is within reach of all users. The second reason for not using EEG together with DBS is that DBS-induced electrical noise can completely obscure the neural activity of interest (Fig. 2). This second limitation poses more of a problem,

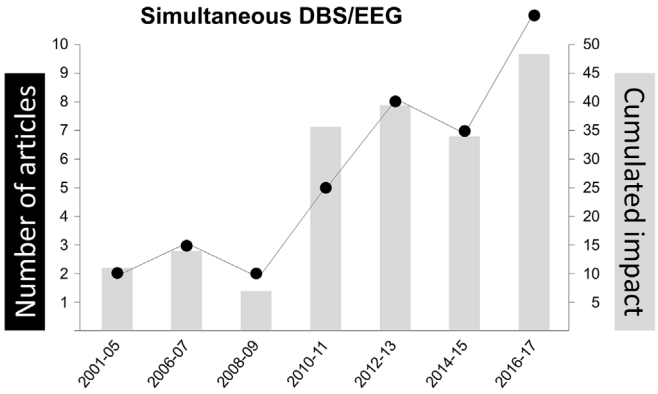

Fig. 1. Growing interest for using EEG to study the effect of STN-DBS on cortical activity, as evidenced by the increasing number of publications in ISI journals and the increasing impact of these studies (cumulated impact = sum of the individual 2014 Journal Citation Reports® impact factors for the corresponding period).

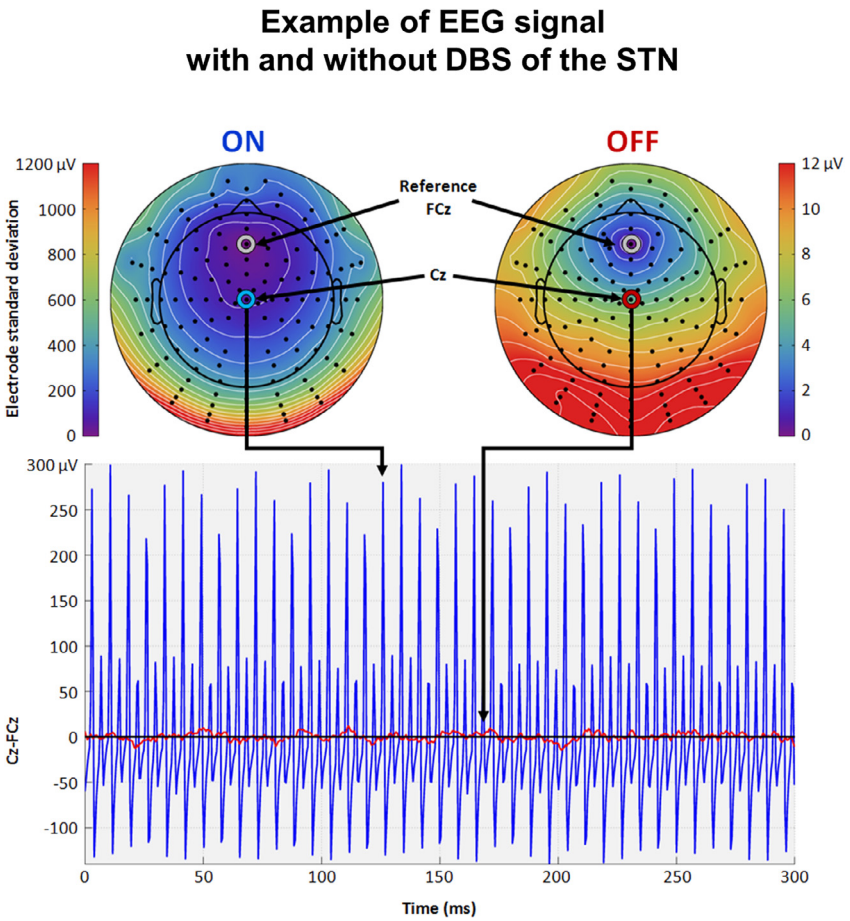

Fig. 2. Topographical and Cz-FCz time-course representations of the effect of STN-DBS on the variance of the EEG signal for one representative parkinsonian patient. Data were acquired with the Biosemi Active Two Mk2 amplifier (Sampling rate: 2048 Hz; Digitalization: 24bit, 4th order Delta-Sigma modulator, 64× oversampling; Input range: −262 mV to +262 mV). DBS induced artifacts are broadcasted on all electrodes of the scalp, with a signal/noise ratio higher than 1×10^{-3} (−40 dB; $10 \times \text{Log10}\,(12^2/1200^2)$), as estimated with an amplifier with a low pass response below ~400 Hz).

and the available methods for filtering DBS artifacts are neither easy to use nor fully effective at removing the artifacts (see Erez et al., 2010 for a generalized framework for stimulus artifact removal in electrophysiological recordings). Here, we provide a critical review of the existing solutions, together with a user-friendly and open-source toolbox for combining and optimizing the use of these different techniques.

2. DBS artifacts: What do they consist of and why are they so difficult to remove?

Clinically effective, high-frequency DBS consists in delivering to the targeted structure a train of narrow pulses (60 µs to ~200 µs), with an amplitude greater than 1 V, at a frequency greater than ~100 Hz. This signal is volume-conducted to the scalp, where it produces large artifacts relative to the scale of neural activity measured using typical electroencephalographic recording devices (10^{-6} Volt, Fig. 2). Intuitively, this may not appear to be a serious problem since DBS is applied at a single frequency, which implies that standard analog or digital filters could remove DBS-induced artifacts. Unfortunately, dealing with DBS-induced artifacts is more complex than simply considering the stimulation frequency (Erez et al., 2010), and these artifacts actually affect the entire frequency spectrum, including many physiologically relevant frequency bands. We propose a brief description of the nature and mechanisms of generation of these artifacts before examining the characteristics and limitations of the available filtering methods.

2.1. The sampling bias during analog to digital conversion (aliasing effects)

Recording a continuous physical quantity with a computer device requires that this quantity is converted into a digital signal by sampling at discrete intervals of time. This step is achieved using an analog to digital (A/D) converter, which samples the signal at a predefined frequency. How high should this frequency be to ensure a faithful representation of the continuous EEG signal? In principle, no information is lost in the sampling process if the sampling rate is at least twice the highest frequency in the signal of interest (Nyquist, 1928; Shannon, 1949). However, when the DBS signal is mixed with the EEG signal, the question also arises as to how high should the acquisition frequency be to ensure a faithful representation of the DBS signal? This is not a trivial question because the original signal of DBS pulses is a spike-train in the time domain, i.e., a square wave containing odd frequency harmonics, not a sinusoidal signal as the EEG signal (Fig. 3A). In theory, an extremely high (infinite) sampling rate is thus required to ensure a faithful recording of the DBS signal. In practice, DBS pulses are regularly missed or badly captured by the A/D converter that is limited in its acquisition frequency and amplitude range (Fig. 3B). The probability that a DBS pulse is missed or distorted during recording depends on several factors including the sampling frequency, the type of A/D converter, the DBS frequency, the DBS pulse width and the phase between the DBS signal and the sampling function, the desynchronization between the internal clocks

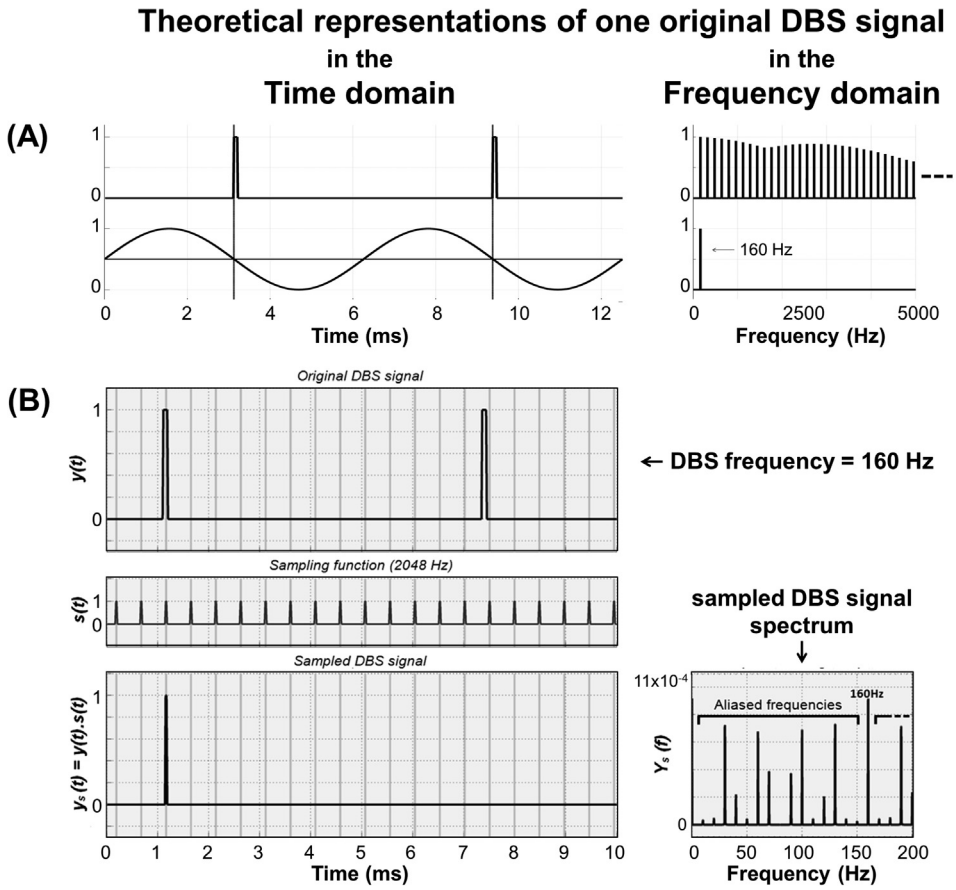

Fig. 3. Simulation of time domain (left side) and frequency domain (right side) representations of one typical DBS signal (160 Hz, pulse width 60 μs, upper part). **A-**The DBS signal is a spike-train of square signals in the time domain (upper part). In the frequency domain (after fast Fourier transform), the signal is composed of an infinite number of harmonics (only shown up to 5 kHz). Only a 160 Hz sinusoidal signal is made of a single fundamental frequency at 160 Hz without harmonics (lower part). **B-**When the same DBS signal is sampled at 2048 Hz by an A/D converter (left side), the sampling function regularly misses some spikes in the time domain. This creates artifactual signals in the frequency domain, both below and above the fundamental harmonic (aliasing, right side).

of the stimulation and the recording devices. These measurement errors have their own period, leading to artifactual values outside the range of the actual DBS frequency, the so-called aliasing effect (Fig. 3). Moreover, even if the sampling rate is sufficiently high to measure each of the successive peaks in the signal, the jitter between the clocks of the recording and the stimulation devices is further responsible for a non-negligible part of the aliasing effect. Critically, aliased frequencies can contaminate all frequency bands, including frequencies well below the frequency of stimulation (Allen et al., 2010; Jech et al., 2006; Sun et al., 2014).

2.2. The filtering bias after data acquisition

A common solution for suppressing artifacts during post-acquisition data processing consists in removing the whole activity contained within the noisy frequency bands. An efficient filter, however, requires that only the noise component at each interference frequency is removed, and that the actual EEG signal content in this frequency band is preserved. It is essential, especially for growing spectral analyses, because the EEG frequency-specific signals provided by time-frequency examination have the potential to disentangle various processes that are known to operate in specific frequency bands (e.g., Albares et al., 2014; Makeig et al., 2004; Siegel et al., 2012). Yet, it could be argued that suppressing the whole signal in the high gamma range (the DBS range) does not matter if the frequencies of interest are below the cut-off. Of course, that only holds if DBS artifacts apply strictly at or above the actual DBS frequency, which is not the case (e.g., Jech et al., 2006; Santillán-Guzmán et al., 2013). The filtering problem thus remains complex yet classical: Using a filter that discriminates between signal and noise.

Within this context, we propose a systematic review to identify and evaluate the techniques available for filtering DBS artifacts from the EEG.

3. Systematic review

We searched the Web of Science and Pubmed databases using the keywords (“EEG” OR “Electroencephalograph* ”) AND (“DBS” OR “Deep Brain Stimulation”).[1] All human scalp EEG empirical studies during clinically effective high frequency DBS published before 2018 were considered, including methodological studies providing real human data. The analysis returned thirty seven studies, mostly published during the five last years (~57%). For each study, we assessed: (1) the overall strategy appropriated by the authors for removing DBS-induced artifacts, (2) the characteristics of the EEG device/digitization procedure (e.g., sampling rate, A/D converter’s internal antialiasing filter, etc.), and (3) the characteristics of the off-line digital filtering procedure (e.g., bandpass filtering, Hampel filtering, etc.). Detailed results are presented in Table 1.

In five studies (13%), the issue of removing DBS artifacts was not mentioned, and no specific filtering was implemented. In nine

[1] And all related terminologies.

Table 1
Technical solutions identified in the systematic review of all empirical studies published before January 2016 using EEG recordings during clinically effective high frequency DBS in humans.

Study		Overall strategy	EEG device/Analog solutions			Offline filtering/Digital solutions				Other
Authors	year		Model	Analog anti-aliasing filter	A/D conversion	Band pass digital filtering	Frequency domain filtering			
							Notch filtering (man.)	Hampel filtering	Matched filtering	
Casula et al.	2017,	Unknown	BrainAmp 32MRplus, BrainProducts	Unknown	5000 Hz	Band pass 0.1–1000 Hz	no	No	No	No
Durschmid et al.	2017	Notch filters	unknown	Unknown	256 Hz	Band pass 1–40 Hz	20 and 50 Hz + 3 harmonics	No	No	No
Kibleur et al.	2017	Notch filters	Acticap, Brain Products	Unknown	2500 Hz resampled at 250 Hz	Band pass 0.6–40 Hz + low pass 30 Hz	Centered on the main harmonics of the stimulation artifact	No	No	No
Kim et al.	2017	Unknown	GRASS Technologies Corporation	Unknown	200 Hz	Unknown	No	No	No	No
Miocinovic et al.	2017	Negligeable scalp artifacts (considered as confined to frequencies above 50 Hz)	Biosemi ActiveTwo System	Yes but unknown characteristics	2048 Hz	High pass at 1 Hz	No	No	No	No
Magrassi et al.	2016	Unknown	SystemPLUS, Micromed	Unknown	2018 Hz	Band pass 1–40 Hz	No	No	No	No
Mideksa et al.	2016	Notch filter	Simultaneous MEG/EEG (Elekta Neuromag)	Unknown	2500 Hz	Unknown	Centered on DBS frequency (125–135 Hz)	No	No	No
Mückschel et al.	2016	ICA + digital low pass filtering	Unknown	Unknown	Unknown	Band pass 0.5–20 Hz	No	No	No	Rejection of artefactual ICs after visual inspection
Scholten et al.	2016a	Negligeable scalp artifacts (bipolar DBS)	BrainVision, Brainproducts	Unknown	1000 Hz	Band pass 1–200 Hz	No	No	No	Bipolar DBS
Scholten et al.	2016b	Unknown	BrainVision, Brainproducts	Unknown	Unknown	Band pass 1–200 Hz	No	No	No	No
Sun and Hinrichs	2016	Pulse detection in the temporal space and template subtraction	Walter Graphtek EEG recorder	Unknown	512 Hz	Band pass 0.5–180 Hz	No	No	No	Offline up-sampling, DBS pulse detection, moving average template subtraction with re-sampling.
Gulberti et al.	2015a	ICA + digital low pass filtering	BrainAmp, Brainproducts	Unknown	1000 Hz	Low pass < 100 and 48 Hz for time–frequency and power spectrum, respectively	No	No	No	Rejection of artefactual ICs after visual inspection
Gulberti et al.	2015b	ICA + digital low pass filtering	BrainAmp, Brainproducts	Unknown	1000 Hz	low pass < 30 Hz	No	No	No	Rejection of artefactual ICs after visual inspection
Markser et al.	2015	negligeable scalp artifacts (bipolar DBS)	Unknown	Unknown	Unknown	Unknown	No	No	No	No
Sun et al.	2015	Matched filters + notch filters	Synamp2, Neuroscan	Unknown	1000 Hz	Low pass < 100 Hz	Yes	No	Yes	No
Weiss et al.	2015	Negligeable scalp artifacts (bipolar DBS)	BrainAmp, Brainproducts	Unknown	1000 Hz	Band pass 0.5–200 Hz	No	No	No	Bipolar DBS
Quraan et al.	2014	Digital low pass filtering	NeuroScan SynAmps	Low-Pass at 3.5 kHz	1000 Hz	Band pass 2–20 Hz	No	No	No	Bipolar DBS
Sun et al.	2014	Matched filters	Synamp2, Neuroscan	Unknown	1000 Hz	band pass 0.3–200 Hz	Yes	No	Yes	No
Figee et al.	2013	Digital low pass filtering	Advanced Neuro Technology	Unknown	512 Hz	Band pass 0.5–40 Hz	No	No	No	No
Hohlefeld et al.	2013	Digital low pass filtering	NeuroScan SynAmps	Low-Pass at 3.5 kHz	2000 Hz	Low pass < 30 Hz	No	No	No	No

Table 1 (*continued*)

Study		Overall strategy	EEG device/Analog solutions			Offline filtering/Digital solutions				Other
Authors	year		Model	Analog anti-aliasing filter	A/D conversion	Band pass digital filtering	Frequency domain filtering			
							Notch filtering (man.)	Hampel filtering	Matched filtering	
Santillan-Guzman et al.	2013	EMD detrending and manual artifacts rejection by TFDF	Unknown	Unknown	1000 Hz	no	yes	no	no	TFDF
Selzler et al.	2013	Digital low pass filtering	NeuroScan SynAmps	Low-Pass at 3.5 kHz	1000 Hz	Band pass 0.5–50 Hz	No	No	No	No
Muthuraman et al.	2012	Oversampling + spatial filtering	Unknown	Unknown	Unknown	No	No	No	No	Iterative DICS
Walker et al.	2012a	Oversampling + differential ERPs (Bipolar stimulation)	Unknown	Low-Pass at 3 kHz	10,000 Hz	No	No	No	No	Yes (DBS ERP)
Walker et al.	2012b	Oversampling + differential ERPs (Bipolar stimulation)	Unknown	Low-Pass at 3 kHz	10,000 Hz	no	no	no	no	Yes (DBS ERP)
Weiss et al.	2012	digital low pass filtering	NeuroScan SynAmps	Low-Pass at 3.5 kHz	1000 Hz	FIR 1–100 Hz + notch 50 Hz	No	No	No	No
Cavanagh et al.	2011	Digital low pass filtering	NeuroScan SynAmps	Low-Pass at 3.5 kHz	1000 Hz	low pass at 50 Hz	No	No	No	No
Swann et al.	2011	Digital low pass filtering	Biosemi ActiveTwo System	Low-Pass first order at 3.6 kHz (3 dB)	2048 Hz - resampled at 512 Hz	low pass at 50 Hz	No	No	No	No
Allen et al.	2010	Digital filtering + automatic outlier frequencies suppression	NeuroScan SynAmps	Low-Pass at 3.5 kHz	1000 Hz	low-pass at 100 Hz, 8th order type II Tchebychev filter, attenuation 40 dB in the stop band.	No	Yes	No	No
Klostermann et al.	2010	Averaging (standard ERP study)	Unknown	Unknown	2000 Hz	band pass 0.05–500 Hz	No	No	No	No
Weiss et al.	2011	Negligeable scalp artifacts (bipolar DBS)	BrainAmp, Brainproducts	Unknown	5000 Hz – resampled at 1000 Hz	band pass 1–100 Hz	No	No	No	Bipolar DBS
Moll et al.	2009	High resolution time/ frequency transform	AlphaMap, Alpha-Omega	Low-Pass at 10 kHz	3000 Hz	band pass 1–300 Hz	No	No	No	No
Kovacs et al.	2008	Averaging (standard ERP study)	Cambridge Electronic Devices Inc. Power 1401 A/D converter	Low-Pass at 500 Hz	1000 Hz	band pass 0.3–30 Hz, 4th order Butterworth IIR filter	No	No	No	No
Colloca et al.	2006	Digital low pass filtering	Unknown	Unknown	256 Hz	band pass 6.5–55 Hz	No	No	No	No
Frysinger et al.	2006	Negligeable scalp artifacts (bipolar DBS)	Unknown	Unknown	unknown	unknown	No	No	No	Bipolar DBS
Jech et al.	2006	Manual detection and suppression of DBS and aliased frequencies in the frequency domain	Brainscope (M&I)	Unknown	250 Hz/ 1000 Hz	band pass 0.015–75 Hz/300 Hz	Yes	No	No	No
Silberstein et al.	2005	Negligible scalp artifacts (bipolar DBS)	Biopotential Analyzer Diana	Unknown	184 Hz	no	No	No	No	Bipolar DBS
Priori et al.	2001	Averaging (standard ERP study)	Unknown	Unknown	Unknown	Unknown	No	No	No	No

DBS = Deep Brain Stimulation; EMD = Empirical Mode Decomposition; TFDF = Time Frequency Domain Filter; DICS = Dynamic Imaging of Coherent Sources.

studies (23.7%) the authors considered DBS artifacts negligible (most often for bipolar DBS and standard ERP studies), and no specific filtering was implemented. In eight studies (21%), a single digital low-pass filter was used to analyze cortical activity in a frequency band lower than the stimulation frequency. In these latter two groups of studies, the possibility of aliasing was ignored. Nine studies (23.7%) considered the aliasing effect and used more sophisticated methods tracking outliers in the frequency domain to identify and remove DBS artifacts above and below DBS the frequency (manual detection and rejection using notch filters, Hampel filtering, matched filters). Three studies (7.9%) combined digital low-pass filtering with independent component analysis (ICA) to identify DBS artifacts as independent components of the EEG signal. Finally, three studies (7.9%) used strategies relying on data acquisition oversampling to allow a more specific analysis of the cortical activity evoked by the stimulation pulse (Muthuraman et al., 2012; Walker et al., 2012a,2012b). In these studies, specific methods were used to dissociate the cortical signal from the artifactual signal in space (Muthuraman et al., 2012) or in time (Walker et al., 2012a,2012b).

4. A/D solutions

4.1. Over-sampling

Oversampling is a theoretically sound strategy to reduce aliasing (Fig. 4), but it is practically limited. EEG sampling rate is limited by several factors, especially the number of channels that have to be acquired simultaneously. For instance, the popular Biosemi Active 2 system is limited to a sampling rate of 2048 Hz at the output for 256 electrodes, 4096 Hz for 128 electrodes, 8192 Hz for 64 electrodes, etc. Indeed, the studies identified above that use a sampling rate of 10,000 Hz recorded from no more than 16 electrodes, which poses a serious problem for EEG studies where high density EEG (64–256 channels) is required to perform accurate separation and localization of electrical sources (e.g., Michel et al., 2004).

Oversampling is unquestionably beneficial for any step of the A/D conversion as well as post-acquisition processing, and the maximum sampling rate should be systematically used before any attempt to filter high frequency DBS artifacts. However, aliasing effects do not vanish at affordable sampling frequencies (Fig. 4), meaning that high sampling is necessary but not sufficient. Future high-resolution EEG systems with sampling frequencies above 10 kHz/128 channels, along with data processing facilities, will be an important advance for the field.

4.2. Analog low-pass antialiasing filters

Almost all recording devices with an A/D conversion step use analog lowpass filters to reduce aliasing effects. These filters are designed to suppress all frequencies above the half of the sampling frequency (the so-called Nyquist-Shannon frequency). The goal is to limit saturation of the analog modulator of the A/D converter and to avoid frequencies above the half of the sampling rate being aliased into the bandwidth of interest. In practice, such filters can distort the signal of interest, are limited in their complexity (filter order), are better suited to filter very high frequencies (~5 kHz) and should not interfere with the oversampling capacity of modern

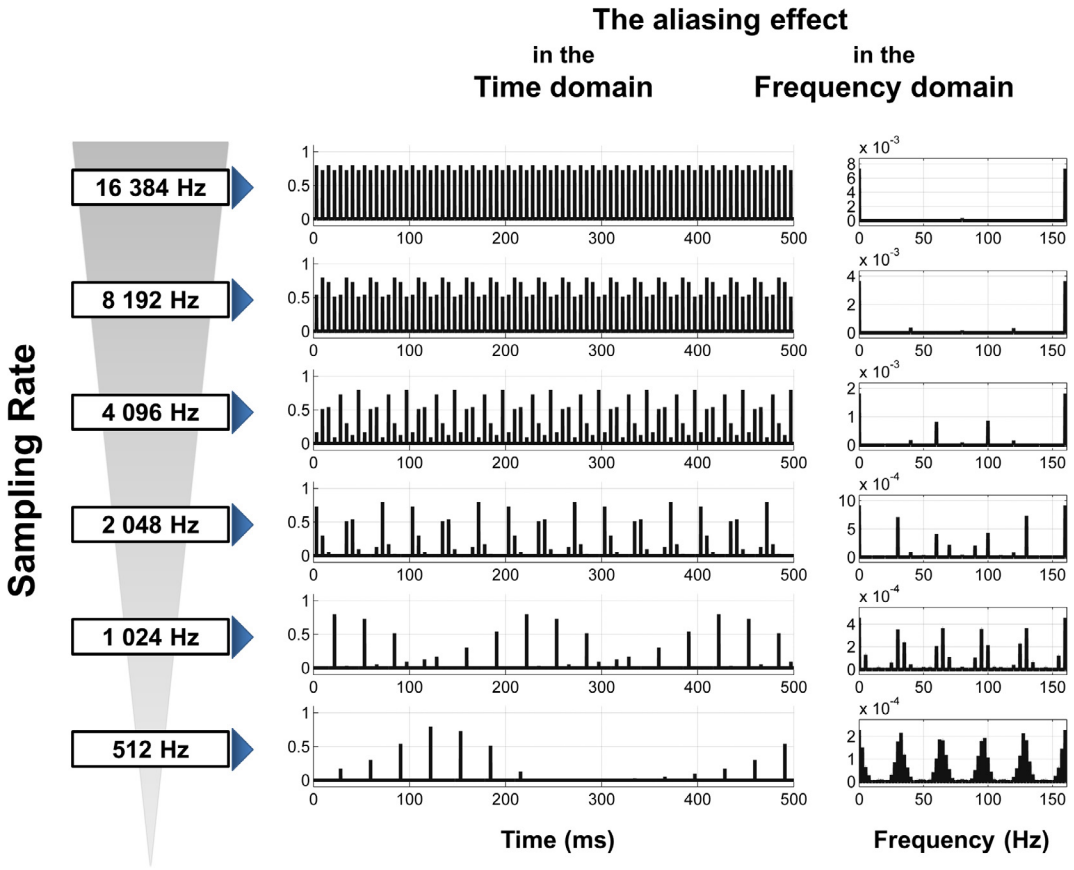

Fig. 4. Simulation of the aliasing effect for different sampling rates. The same typical DBS signal is used (160 Hz, pulse width 60 μs, upper part). The simulation includes the effect of the antialiasing analog filter (see Figs. 5 and 6). The lower the sampling rate; the higher the number of spikes missed in the time domain, and the higher the number of aliased frequencies in the frequency domain. Residual distortions are observed even for unconventionally high sampling frequencies.

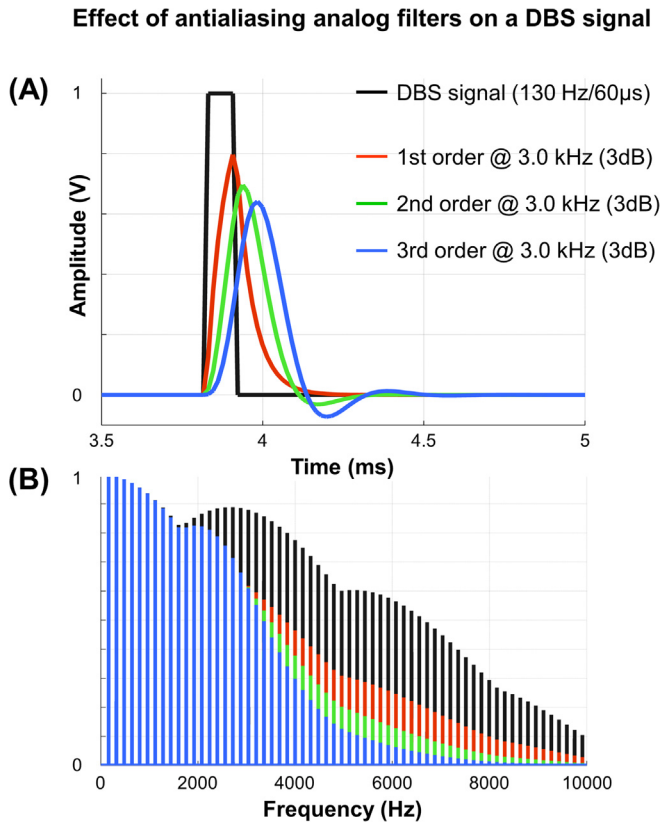

Fig. 5. Illustration of the effect of an antialiasing Butterworth analog filter on a DBS signal (identical parameters as in Fig. 4 are used for this simulation). **A-** The effect on the amplitude of the signal is limited, but the signal is delayed and distorted (the effect increases as the order of the filter increases). This illustration also introduces another problem related to the bias generated by such analog filters for the analysis of DBS-induced event-related potentials (e.g. Baker et al. 2002; MacKinnon et al. 2005; Walker et al. 2012a, 2012b). **B-** Antialiasing analog filters do not completely solve the problem because the DBS transformed signal is still a complex mixing of harmonic components below the cut-off frequency.

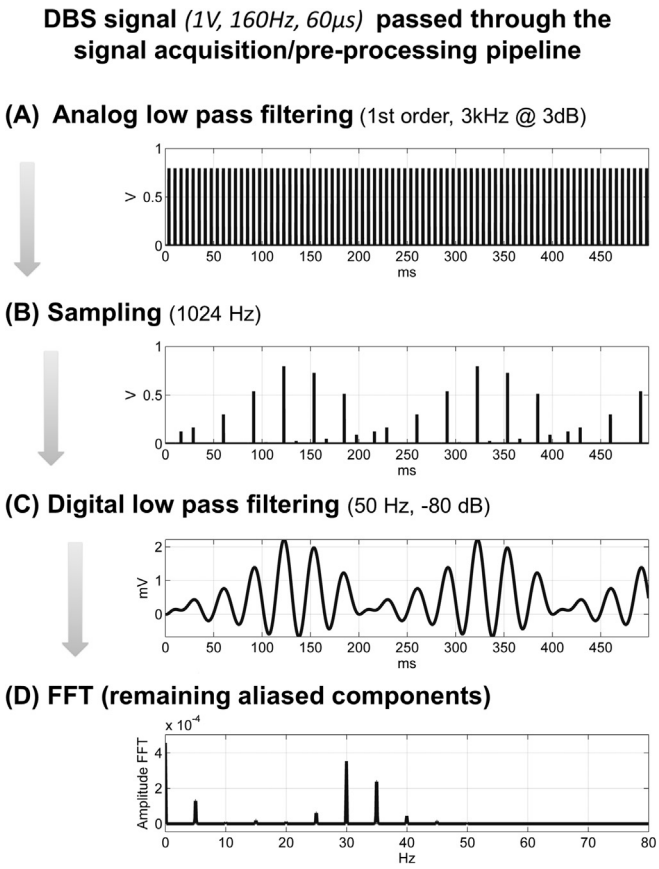

Fig. 6. Illustration of a 1 V, 160 Hz, 60 µs DBS signal passed through the whole signal acquisition/pre-processing pipeline. **A-** Analog antialiasing filter (Butterworth, First order, Low pass at 3 kHz, 3 dB). The signal amplitude is slightly attenuated, but remains equivalent to a spike train at the stimulation frequency (see Fig. 5). **B-** A/D conversion (sampling rate 1024 Hz). The sampling frequency is too low to adequately capture the DBS signal (aliasing effect, see Figs. 3 and 4). **C-** Offline digital filtering (Two pass, zero-phase, Low pass Chebyshev type II at 50 Hz, Attenuation 80 dB in the stop band.). High frequency components are effectively removed, but a smoothed periodic signal, with an amplitude of more than 2 mV remains. **D-** High resolution amplitude spectrum of the remaining signal. The artifact is composed of harmonics of the stimulation frequency, aliased in the frequency band of interest. Such signal can bias spectral and coherence analyses in low frequency bands and must be removed.

A/D converters. Accordingly, these filters are often single pole low pass filters with a cutoff frequency of 3 dB around 3 kHz (Table 1, Fig. 5), far above the fundamental frequency of DBS. Therefore, these filters have a very limited effect on DBS-induced artifacts (Figs. 5, 6).[2] Fig. 7 shows real data illustrating the fact that artifacts in low frequency bands remain after antialiasing solutions such as analog low-pass filters and oversampling/delta-sigma modulation for A/D conversion. Indeed, these methods are not designed to remove artifacts with a magnitude comparable to that induced by DBS (estimated signal/noise ratio>>−30 dB, Fig. 2).

5. Digital solutions

5.1. Low-pass filtering

Digital filters can be applied online during data acquisition, and/or offline after the whole signal has been recorded. Digital filters are typically used in data acquisition systems to remove the noise injected during the A/D conversion. Such filters have a cutoff frequency far above the frequency band of interest to limit phase distortions at lower frequencies. Accordingly, offline zero-phase low-pass filters with a cutoff frequency below the stimulation frequency are necessary to remove most of the artifacts induced by high frequency DBS. Digital filters have better properties than analog filters, with a sharper roll off and a good attenuation in the stop band. All frequencies above the stimulation frequency are removed with this procedure, but aliased frequencies below the cut-off will remain unchanged. In the temporal domain, the resulting signal is a smoothed periodic signal (Fig. 6) mixed with the actual neurological signal.

Many of the studies we examined applied low-pass filters alone to remove DBS artifacts (e.g., Cavanagh et al., 2011; Figee et al., 2013, etc., Table 1), assuming that DBS-induced high-frequency signals will simply be suppressed from the mixed set of signals recorded at electrodes sites. This is justified if the sampling rate is sufficiently high to avoid any aliasing phenomenon, but in practice the sampling rate is always too low and the magnitude of the DBS-induced electrical noise is too high to neglect aliased frequencies (Jech et al., 2006; Allen et al., 2010). Digital low-pass filtering does not compensate for analog filtering limitations, which was clearly demonstrated by Santillán-Guzmán et al. (2013) who showed that the power spectrum of the low-pass filtered signal in the ON state remains contaminated by comparison to the OFF state control condition. Even with high-performance equipment,

[2] More information about the physical properties of the analog filter can be found in datasheets issued from the semi-conductor industry (e.g. Baker 1999, Antialiasing, Analog filters for Data acquisition systems, AN699 Microchip Technology Inc).

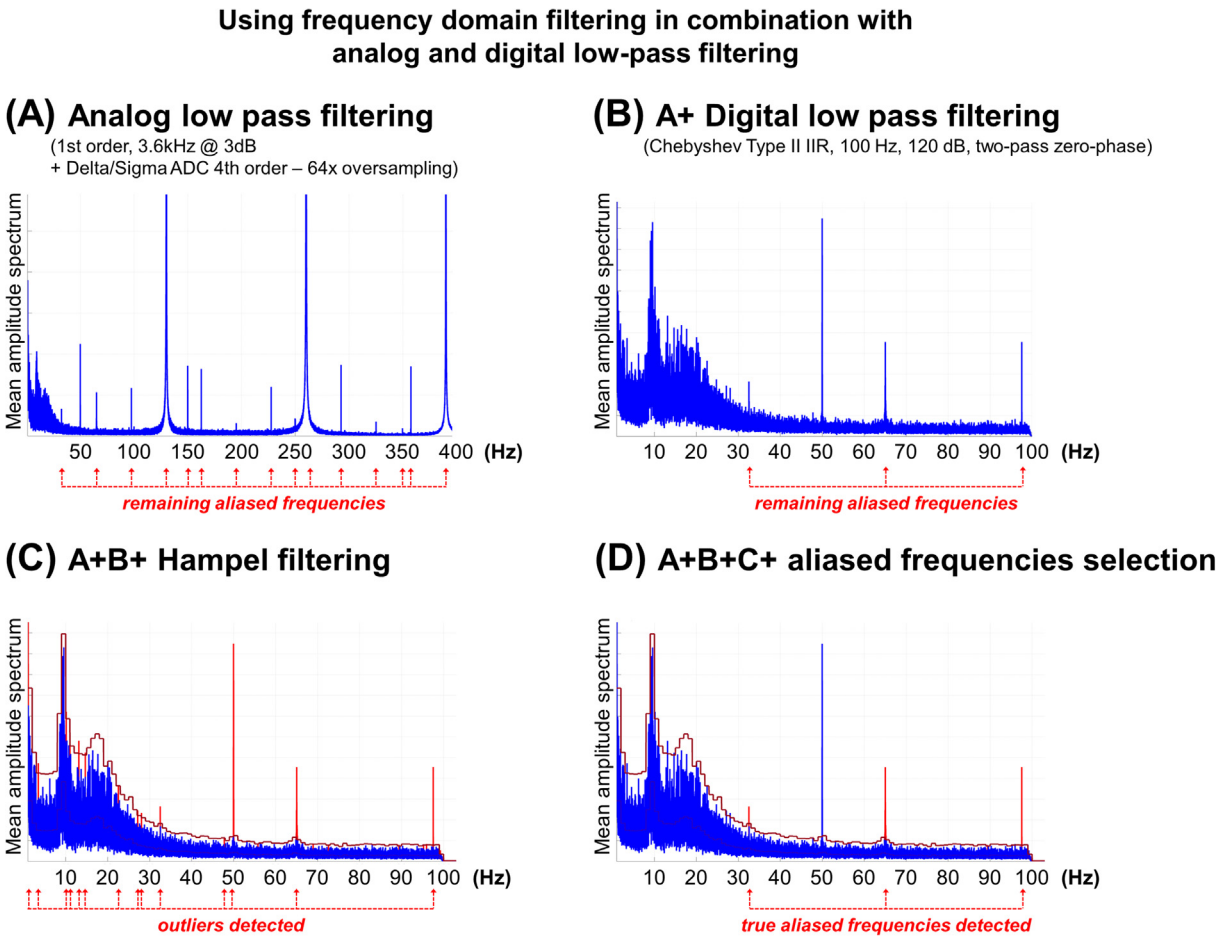

Fig. 7. Illustration in the frequency domain of the respective effects of the different existing methods for filtering DBS artifacts (Real data). Data were recorded at 2048 Hz from one Parkinsonian patient (152 seconds resting state, eyes closed), with STN DBS delivered at 130 Hz (Left, 3.2 V, 60 μs; Right, 3.0 V, 90 μs), with an EEG device using an analog low pass filter and an oversampling strategy to limit the aliasing effect (BiosemiActiveTwo Mk2 amplifier, Sampling rate: 2048 Hz; Digitalization: 24bit, 4th order Delta-Sigma modulator 64× oversampling; Input range: −262 mV to +262 mV; Low-pass antialiasing analog filter - first order – cutting frequency at 3.6 kHz (3 dB)). **A-** High resolution power spectrum averaged for all electrodes. The fundamental of the stimulation frequency and the two first harmonics are observed at 130, 260 and 390 Hz. Despite the antialiasing features of the high-resolution recording device, aliased frequencies remain. **B-** Same data after low pass filtering (Chebyshev Type II IIR filter, attenuation 120 dB, two-pass zero-phase). Most of the DBS induced artifacts are removed, but aliased frequencies remain in the main frequency bands of interest for EEG analyses. **C-** Automatic detection of outliers in the high resolution power spectrum by the Hampel identifier (dark red line; windows length: 1 Hz; threshold: 2). All frequencies above the Hampel identifier are deemed as artifacts, whenever they are actual aliased frequencies or not. **D-** Same data after identification of aliased spikes. Only spikes above the Hampel identifier which are sub-multiple of the stimulation frequency are deemed as artifacts and interpolated. As a consequence, powerful low frequency neuronal activity spiking above the Hampel identifier are no longer erroneously considered as artifacts in this example. Obviously, the same applies to the 50 Hz powerline, which must be filtered separately. (For interpretation of the references to colour in this figure legend, the reader is referred to the web version of this article.)

simple low-pass temporal filtering is not satisfactory to remove DBS-induced artifacts (Fig. 7).

5.2. Frequency-domain filtering

DBS-induced electrical signal can be assumed as being stationary, i.e., the power spectrum and the phase of the signal that has to be removed are not supposed to change over time. If this assumption is correct, suppressing the remaining low-frequency artifacts after low-pass filtering can be performed by means of frequency-domain filtering techniques since aliased artifacts appear as distinct peaks throughout the frequency spectrum. There are several solutions, but relatively few studies have used this kind of technique (only six were identified in our systematic review, Table 1). It can be implemented by manual detection of the aliased frequencies in the high resolution power spectrum of the data, and application of a set of specifically designed band-stop filters (Jech et al., 2006). A variant of this method based on a hybrid (time/frequency) filtering strategy has later been proposed by Santillán-Guzmán et al. (2013), which is useful when a clear and narrow peak at the stimulation frequency cannot be easily detected in the high resolution power spectrum (i.e. when the stationary assumption has been violated).

However, this kind of technique needs time-consuming and expert analysis of the data, and relatively complex signal processing procedures to preserve the neurological signal around the aliased frequencies. Allen et al. (2010) propose an automatic method to circumvent this problem. After the time-domain signal has been transformed into the frequency domain with the fast Fourier transform (FFT), a Hampel filter is used to identify artifactual frequency peaks, and these peaks are replaced with interpolated values. The Hampel filter is a robust statistic that detects outliers in a sequence as those data points for which the difference from a locally estimated median is greater than a pre-determined threshold (Fig. 7). The cleaned spectrum is then transformed back to the time domain via the inverse FFT. This original method represents a major advance, not only because it can detect aliased frequencies, but also because it has the potential to remove only the noise component at each interference frequency, i.e., to preserve the actual EEG signal in this frequency band. However, for

two main reasons, it is less popular than low-pass filtering methods. First, it requires advanced skills in signal processing since there is no user friendly tool for applying these filters. Second, it requires tuning to avoid over-aggressive filtering and a correct detection of the aliased frequencies (Fig. 7C).

Finally, a more recent technique derived from the understanding of the DBS artifact waveform has been proposed by Sun et al. (2014). Provided that the artifacts frequencies can be predicted and are uncorrelated with the underlying signal, matched filters can be applied to remove the unwanted components (Sun et al., 2014). Matched filters offer a valuable alternative to more standard Finite Impulse Response (FIR) and Infinite Impulse Response (IIR) notch filters. Indeed, while notch filters are just centered at the frequency of the sinusoid, matched filters use both the amplitude and phase information of the sinusoidal component for estimation and removal (Kay, 1993). Theoretically, they are better suited for removing DBS-induced artifacts from the EEG signal than other filters, which are less appropriate because of (i) their inability to estimate automatically the strength of the unwanted component (the attenuation of classical FIR and IIR notch filters has to be determined by the experimenter) and (ii) their spectral spread which leads to suppression of surrounding frequencies as well (Sun et al., 2014). Matched filters can be applied by estimating the phase and the amplitude of an unwanted frequency by calculating the cross-correlation between the noisy EEG signal and an artifact component template (ibid).

Obviously, the critical point with frequency-domain filtering techniques is the accuracy with which artifactual frequencies can be identified. Indeed, aliased frequencies are not a simple function of DBS frequency and acquisition rate, but rather comprise a range of frequencies around the expected component frequency (e.g., Sun et al., 2014). The reason is that the Shannon-Nyquist theory used to predict the frequencies of both the natural and aliased harmonics assumes an ideal A/D conversion while in practice EEG devices have non-linear A/D-Converters like Delta-Sigma modulators. Another reason is clock jittering (Sun and Hinrichs, 2016). The internal clock of the stimulation and the recording devices do not have identical resolution, and are not perfectly synchronized. In consequence, even if the sampling rate is high, all stimulation pulses are not measured exactly in the same manner. This leads to low frequency variations within stimulation pulse recordings, and creates artificial low-frequency components at frequencies below the stimulation frequency. In other words, several phenomena may occur in commercial A/D-Converter that can make aliased frequencies difficult to predict, like periodic saturations of the quantizer, periodic quantization noise, clock jitter, etc. (see Pamarti, 2010; Gaggl, 2013; Sun and Hinrichs, 2016). Unfortunately, many of these parameters are often unknown to the user. The relative unpredictability of aliased frequencies has been highlighted in previous papers (e.g., Jech et al., 2006) and is further illustrated in the present review (Fig. 4). Yet, in any case, it is highly recommended to use high resolution measurement techniques to identify aliased frequencies more accurately before removing them with any frequency-domain filtering technique.

6. Other solutions

6.1. The case of bipolar stimulation

It has been suggested that bipolar DBS stimulation produces clinically insignificant artifacts (Frysinger et al, 2006; Silberstein et al., 2005; Quraan et al., 2014). In a (pseudo)-monopolar configuration, the pulse generator serves as the anode and an intracranial contact as the cathode. This configuration generates a long-dipole electrical field. In a bipolar configuration, intracranial electrodes serve both as the anode and the cathode. This configuration generates a short electrical dipole, and thus involves a smaller volume of tissue. Accordingly, it is sometimes believed to generate negligible artifacts (Frysinger et al., 2006). However, as demonstrated in several studies (Baker et al, 2002, MacKinnon et al., 2005; Walker et al. 2012a,2012b), bipolar DBS stimulation does actually produce significant artifacts (Fig. 8). In addition, the scope of this method is limited because most DBS patients undergo monopolar stimulation. Indeed, usually, at the initial programming of DBS parameters, monopolar stimulation is employed. The patient is switched to bipolar stimulation only if an optimal setting (combining pulse width, frequency, voltage, and electrode configuration) is not reached (Wagle Shukla and Okun, 2014).

6.2. Searching for short latency (direct) activation of cortex by DBS

Studies interested in how DBS synchronizes cortical activity to the stimulation frequency are a special case, and need specific solutions for filtering DBS artifacts. One consists in implementing analytical techniques that reverse the anode and cathode electrode contacts and sum the resulting pair of potentials evoked by bipolar DBS (Walker et al. 2012a,2012b). This technique requires an extremely high sampling rate during data acquisition.

Another approach is based on the use of head models coupled with beamforming techniques to identify the network which oscillates at the same frequency than the DBS (Muthuraman et al., 2012). The method assumes that the spatial signature of the DBS signal is identifiable with satisfactory resolution, i.e., can be isolated from other sources by means of spatial filters.

6.3. Methods based on DBS pulse detection in the temporal space (template subtraction)

Provided that the amplitude of the stimulation artifact is substantial and the acquisition frequency is sufficiently high, thresholding in the temporal domain can be used to better identify stimulation artifacts. This technique is similar to the template subtraction techniques used to reduce gradient artifacts during EEG-fMRI recordings (e.g. Becker et al., 2005). Sun and Hinrichs (2016) recently proposed a resampling strategy that consists in removing DBS artifacts by subtracting adaptive DBS artifact templates from the contaminated data (Fig. 9). Importantly, the major advantage of this method is that it allows precise reconstruction of the artifact shape without the need to oversample the signal during A/D conversion. According to Sun and Hinrichs (2016), this technique is especially beneficial for analyzing activity in higher frequency bands (gamma activity). However, the method does have potential drawbacks. DBS artifact subtraction requires stimulation based epoching (data alignment on the basis of peak detection). Yet, due to the desynchronization of the internal clocks of the recording and stimulation devices, the technique induces a substantial increase of the number and amplitude of aliased frequencies in lower frequency bands (Fig. 9). In addition, DBS artifact subtraction has a considerable potential to introduce strong biases in the spectral signal, as illustrated in Fig. 9. This was not evidenced in Sun and Hinrichs' original investigation probably because their dataset was weakly contaminated by DBS artifacts (no more than a factor 10). It is much more common for DBS artifacts to reach a factor of 1000 (see Fig. 2). As a consequence, given that the noise introduced in the frequency spectrum by stimulation based epoching increases as a function of artifacts amplitude (Fig. 9), it is likely that the method is less efficient with more noisy datasets. In conclusion the method might be convenient for studies focusing on direct (short-latency) activation of the cortex by the stimulation pulse, or bipolar stimulation, but some caution is advised when data processing is concerned with analyses in the spectral domain.

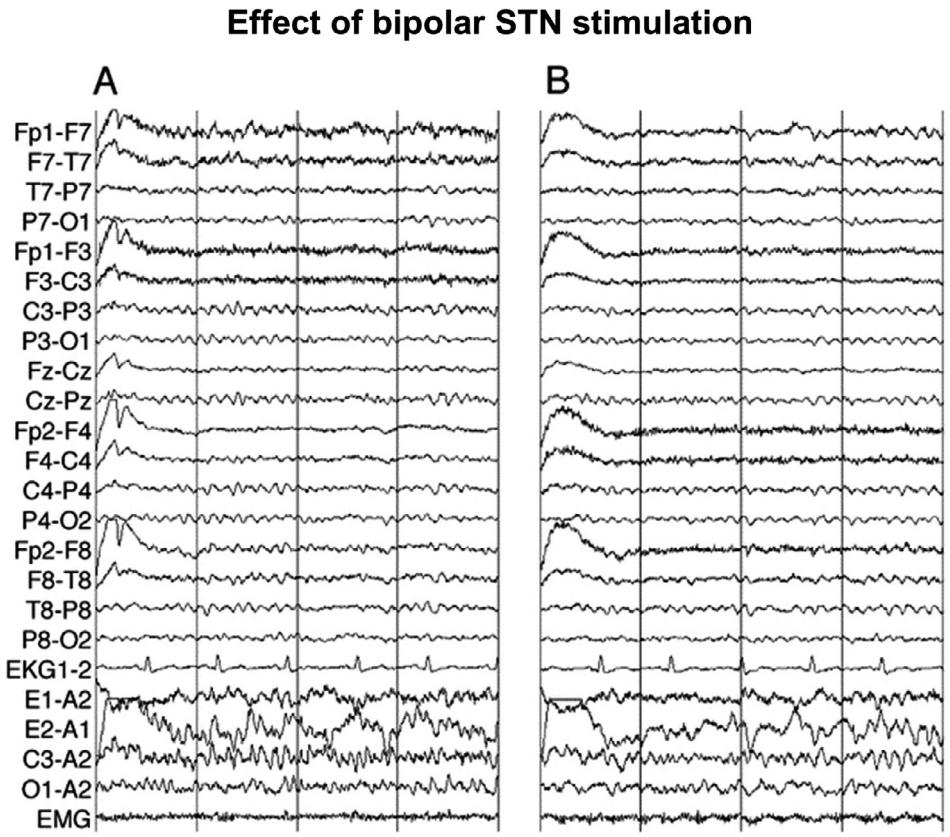

Fig. 8. Four-second excerpts of waking EEG from one subject with bilateral subthalamic nuclear (STN) deep brain stimulation (DBS) for Parkinson disease. (A) Bilateral DBS on in bipolar mode. (B) Both DBS implants off. (3.0 V, case +, 0−, 160 Hz, 90 microseconds. Bar = 100 μV; time marks = 1 second). Reproduced with permission from: Frysinger et al. Neurology 2006; 66:268–270. ©2006 by Lippincott Williams & Wilkins.

6.4. Independent component analysis (ICA)

The general strategy assuming that the signature of the DBS signal can be isolated from the other electrical sources with which it is mixed to form scalp potentials DBS (see above Muthuraman et al., 2012) opens up new perspectives regarding the use of spatiotemporal techniques like ICA to optimize DBS artifacts filtering. Three recent studies (Gulberti et al., 2015a, 2015b; Mückschel et al.,2015) paved the way for this solution. ICA is the most popular blind source separation (BSS) method, a data-driven technique that allows the separation of signals from a set of mixed signals contributing to the overall electrical activity recorded on the scalp. Importantly for the present issue, it is performed with no need of information about the sources or the mixing process. As applied to EEG data, ICA most often uses higher order statistics (HOS) to decompose the raw signal obtained from a specific number of electrodes into the same number of statistically maximally independent components (Delorme et al., 2007; Onton and Makeig, 2006). It has long been employed by EEG users to reject artifacts like eye blinks, saccades, cardiac activity and most of the Gaussian noise. Given the efficiency of the method for denoising classical EEG recordings, the method seems applicable in this instance. However, regarding the unfavorable signal/noise ratio between the DBS artifact and the neuronal sources (Fig. 9), more work has to be done to find a solution that preserves the physiological signal when focusing on whole brain dynamics. One particular difficulty with this method is highlighted in Fig. 10, which shows that whatever the properties of the algorithm used for source separation (Lio and Boulinguez, 2013), DBS spikes can still be found in most sources. This demonstrates that the signature of the DBS signal is not easily identifiable as a single -or a set of- independent component-s-.

7. DBSFILT: An open-source matlab toolbox for optimizing artifacts filtering

Studies on the global effect of DBS (i.e., the effect on the whole EEG spectrum which is supposed to mediate the variety of cognitive and sensorimotor processes modulated by stimulation) require rigorous DBS filtering. The considerations above indicate that no single approach can efficiently remove DBS artifacts from the EEG. Rather, we argue that the techniques of data acquisition and data processing examined can be effectively combined. For this purpose, we have developed an open-source toolbox (DBSFILT) that integrates some of the useful methods for filtering DBS artifacts, as well as routines for optimizing their efficacy. DBSFILT is free software, and we aim to continually including new solutions, scripts, databases, commentaries, or any other contributions to promote collaborative development dedicated to providing optimal solutions to removing DBS artifacts. We have conceived DBSFILT as a starting point for contributors to share their techniques and code in order to allow users to choose the most efficient combination of methods according to the specific conditions under which their signal has been acquired.

Some of the useful functions to date for DBS filtering (low-pass filtering, Hampel filtering with aliased spikes identification, matched filters, automatic detection of the DBS pulses in the temporal domain, etc.) are included in DBSFILT with examples (including data from Fig. 7), tutorials, and a graphical user interface for

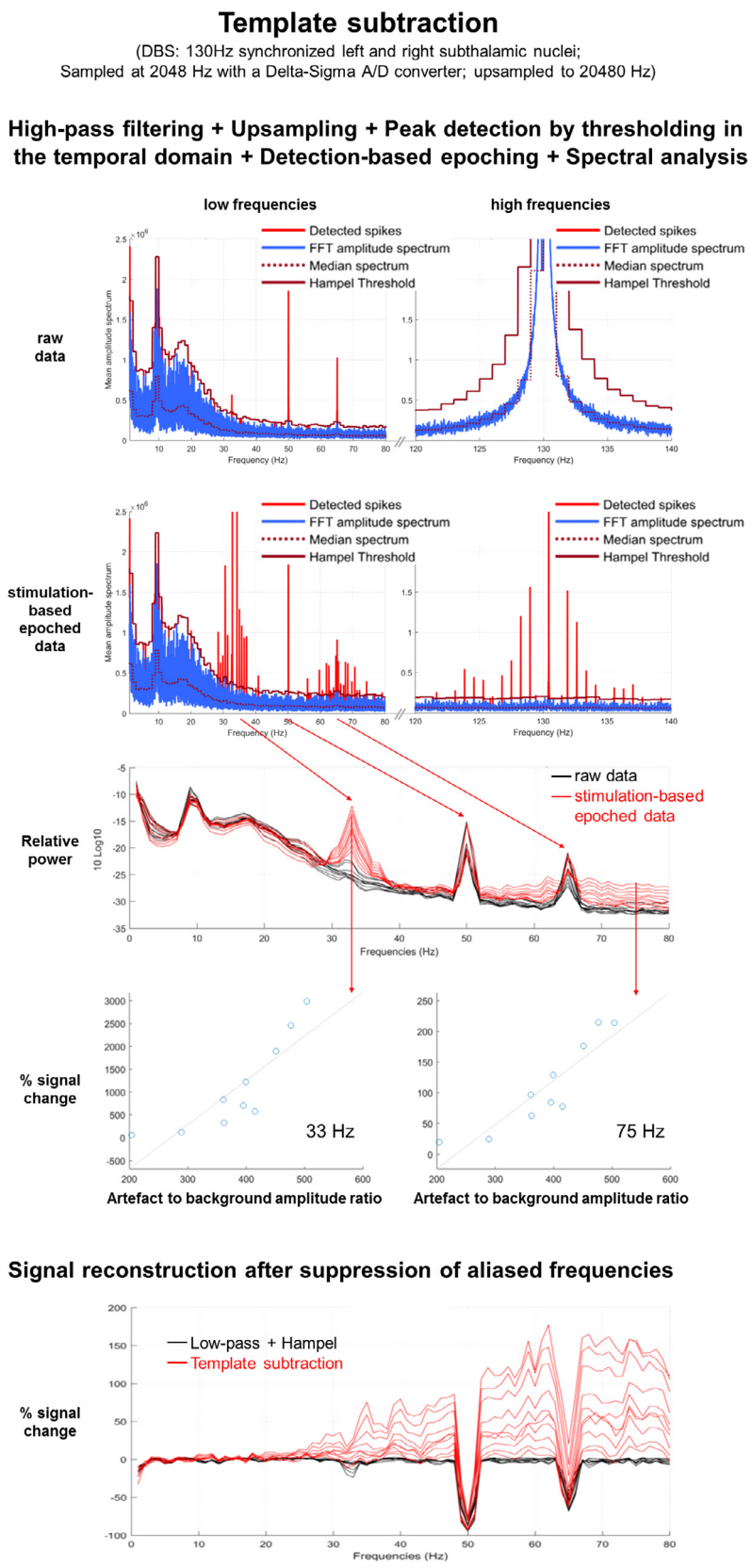

Fig. 9. Moving average template subtraction. (A) High resolution power spectra displayed for raw and aligned signal (re-epoching is based on stimulation peaks detection). The method allows a better definition of the artifact in the high resolution power spectrum around the stimulation frequency. This can be highly beneficial when the stimulation frequency is low and overlaps the frequency band of interest. However, the method can induce substantial increase in the number and amplitude of aliased frequencies in lower frequency bands, as illustrated in the power spectrum of stimulation-based epoched data. Relative power spectral density shows large increases in power due to data alignment, either in the form of increased burst (e.g., 33 Hz) or constant drift (e.g., 75 Hz). The % of signal change after data alignment is strongly correlated with the artifact to background amplitude ratio. (B) Signal reconstruction after moving average template subtraction (red) and low-pass + frequency domain filtering (Hampel)..

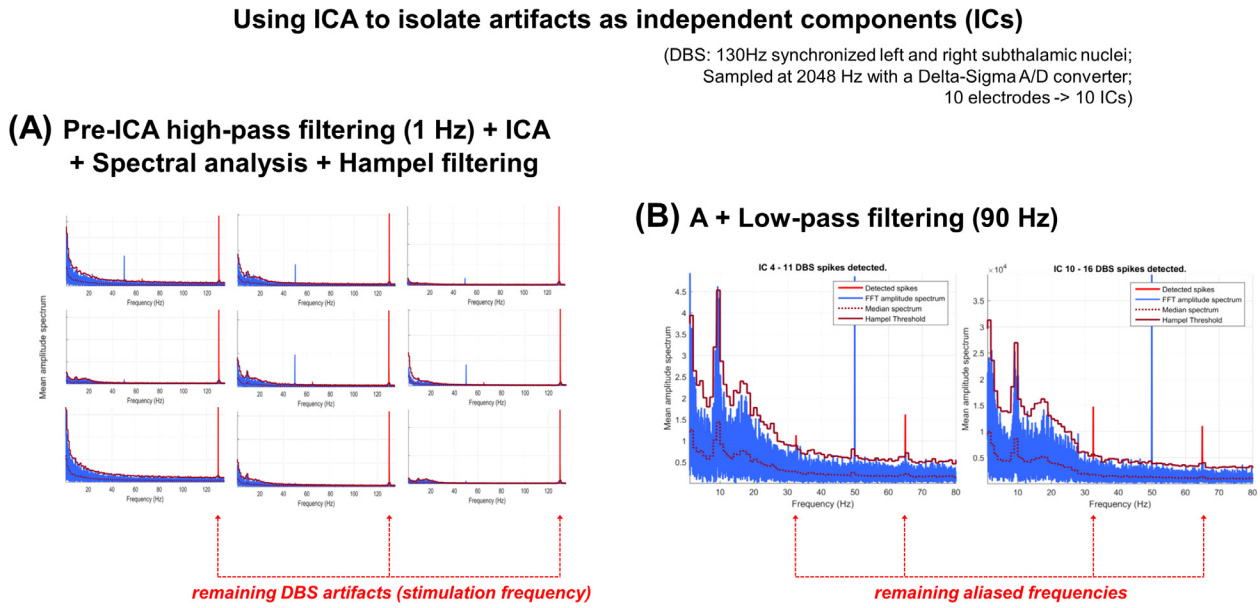

Fig. 10. Using ICA to isolate artifacts as independent components. In this illustration, DBS artifact is not identified as an independent component. (A) When low-pass filtering is not applied, DBS signal is not separated from the other sources, and the powerful 130 Hz peak (DBS frequency) is observed within the mean amplitude spectrum of all sources (only 9 are shown for convenience). (B) When low-pass filtering is applied, aliaised frequencies can still be observed within the mean amplitude spectrum of most sources (6/10, only 2 are shown for convenience).

interactive use. Users can test and combine the different solutions available in order to run the method which best fits the specific needs of their dataset.

This toolbox can be downloaded at:

https://github.com/guillaumelio/DBSFILT/releases

A tutorial can be found on the download platform (technical document: DBSFILT/DBSFILT_GUI_DOC.pdf).

7.1. Example of combination

All methods have advantages and caveats, and below we outline a combined approach and illustrate how it is implemented in our toolbox. We recommend using a mixed approach combining complementary solutions: high sampling rate, analog low-pass filtering, digital low-pass filtering, and frequency-domain filtering guided by artifact identification procedures.

In the method proposed by Allen et al. (2010), the efficiency of the Hampel filter depends on parameters controlling the sensitivity of the filter. As put forward by the authors, the filter is blind. It does not require a priori knowledge of which frequencies to process. Threshold values are determined according to the number and the intensity of the aliased frequencies that can be detected in the high-resolution power spectrum. In other words, setting parameters relies mostly on the characteristics of the data acquisition procedure (sampling rate, A/D conversion) and on the length of the recorded data (spectral resolution). This procedure is convenient because identical parameters are suitable for all subjects, regardless of their individual stimulation parameters. However, this method is often too aggressive and tends to consider as outliers frequency peaks that do not correspond to aliased frequencies (Fig. 7C). In order to avoid this potential bias, we have included a method in the DBSFILT toolbox to guide the filter towards the frequencies at which DBS artifacts are likely to occur. These frequencies are a function of the individual stimulation parameters. Aliased frequencies are typically captured in the high-resolution power spectrum as outlier frequencies that are sub-multiples of the stimulation frequency (Jech et al., 2006, Fig. 7a). The algorithm calculates all possible aliased frequencies and allows automatic removal by the Hampel filter only when the outliers correspond to these frequencies (Fig. 7D):

$$f_{spike} = \boldsymbol{h} \times \left(\frac{f_{DBS}}{n}\right);\ \ where\ \ \boldsymbol{h} = h \pm \varepsilon;\ \ h \in \mathbb{N}^{+}\ \ and\ \ n < n_{max} \in \mathbb{N}^{+}$$

where:

f_{spike} is the outlier frequency detected by the Hampel filter,
f_{DBS} the stimulation frequency,
n the number of consecutive DBS pulses missed (or differently captured (Sun and Hinrichs, 2016)) by the ADC + 1,
n_{max} the estimated maximum number of consecutive DBS pulses missed (or differently captured) by the ADC + 1,
h define the harmonics of the aliased signal,
ε a small number describing the tolerance for DBS spike identification (dealing with the clock accuracy of the sampling and the stimulation device).

Only the stimulation frequency, n_{max} and the ε parameters have to be set by the user (typical values for the A/D and DBS parameters described in the simulations and real data presented in the present paper: $n_{max} = 10°$; $\varepsilon = 0.001$. $n_{max} = 20°$; $\varepsilon = 0.01$).

8. Conclusion

Advanced signal processing methods now make EEG an ideal tool to track brain dynamics with satisfactory spatial resolution and optimal temporal resolution in healthy subjects. However, in patients, removing DBS artifacts from the EEG is currently not straightforward. Our review of the existing methods indicates that no single approach can efficiently remove DBS artifacts from the EEG. Due to the desynchronization between the stimulation and the recording device, aliased frequencies are introduced in the signal. Oversampling is theoretically sound, but sufficient oversampling is currently impossible for high-density EEG. In addition, it is inadvisable to rely on the analog antialiasing filters of EEG

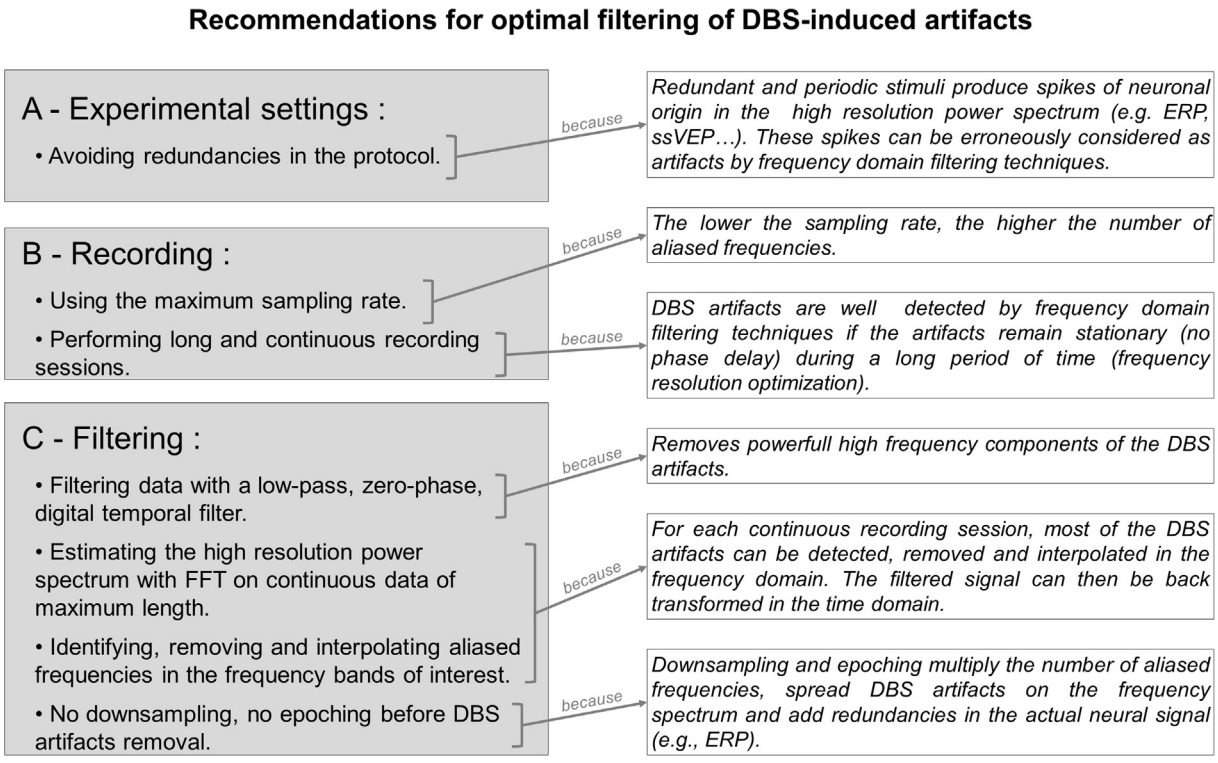

Fig. 11. Issues and recommendations for removing high frequency deep brain stimulation artifacts from the electroencephalogram.

devices because they are not designed to suppress artifacts of such a magnitude. It is also not appropriate to rely on digital low-pass filtering alone since DBS artifacts are also composed of low-frequency components. Frequency-domain filtering techniques are efficient, provided that a routine guiding the filter towards the likely artifactual frequencies is used. However, these methods can be used effectively in combination (oversampling, analogic and digital filtering). Issues and recommendations for an efficient use of these techniques are synthetized in Fig. 11. In any case, any spectral difference observed between ON and OFF stimulation conditions still has to be considered with caution. By offering an open-source toolbox which integrates useful functions for DBS filtering, we hope to stimulate new studies aiming to unravel the controversial nature of DBS effects on whole brain dynamics using EEG.

Acknowledgments

This work was supported by a grant AO-HCL (D50786-UF81431) to Stéphane Thobois, a grant ANR (MNPS-039-01) to Philippe Boulinguez and a grant ANR (ANR-16-CE37-0007-03) to Brian Lau.

Conflict of interest

We declare that we have no conflict of interest.

References

Agnesi F, Johnson MD, Vitek JL. Deep brain stimulation: how does it work? Handb Clin Neurol 2013;116:39–54.
Albares M, Lio G, Criaud M, Anton JL, Desmurget M, Boulinguez P. The dorsal medial frontal cortex mediates automatic motor inhibition in uncertain contexts: evidence from combined fMRI and EEG studies. Hum Brain Map 2014;35:5517–31.
Allen DP, Stegemöller EL, Zadikoff C, Rosenow JM, MacKinnon CD. Suppression of deep brain stimulation artifacts from the electroencephalogram by frequency-domain Hampel filtering. Clin Neurophysiol 2010;121:1227–32.
Aviles-Olmos I, Kefalopoulou Z, Tripoliti E, Candelario J, Akram H, Martinez-Torres I, et al. Long-term outcome of subthalamic nucleus deep brain stimulation for Parkinson's disease using an MRI-guided and MRI-verified approach. J Neurol Neurosurg Psych 2014. https://doi.org/10.1136/jnnp-2013-306907.
Ballanger B, Jahanshahi M, Broussolle E, Thobois S. PET functional imaging of deep brain stimulation in movement disorders and psychiatry. J Cereb Blood Flow Metab 2009a;29:1743–54.
Ballanger B, van Eimeren T, Moro E, Lozano AM, Hamani C, Boulinguez P, et al. Stimulation of the subthalamic nucleus and impulsivity: release your horses. Ann Neurol 2009b;66:817–24.
Baker KB, Montgomery Jr EB, Rezai AR, Burgess R, Lüders HO. Subthalamic nucleus deep brain stimulus evoked potentials: physiological and therapeutic implications. Mov Disord 2002;17:969–83.
Becker R, Ritter P, Moosmann M, Villringer A. Visual evoked potentials recovered from fMRI scan periods. Hum Brain Map 2005;26(3):221–30.
Bourne SK, Eckhardt CA, Sheth SA, Eskandar EN. Mechanisms of deep brain stimulation for obsessive compulsive disorder: effects upon cells and circuits. Front Integr Neurosci 2012;6:29.
Carmichael DW, Pinto S, Limousin-Dowsey P, Thobois S, Allen PJ, Lemieux L, et al. Functional MRI with active, fully implanted, deep brain stimulation systems: safety and experimental confounds. Neuroimage 2007;37:508–17.
Casula EP, Stampanoni Bassi M, Pellicciari MC, Ponzo V, Veniero D, Peppe A, et al. Subthalamic stimulation and levodopa modulate cortical reactivity in Parkinson's patients. Parkinsonism Relat Disord 2017;34:31–7. https://doi.org/10.1016/j.parkreldis.2016.10.009.
Cavanagh JF, Wiecki TV, Cohen MX, Figueroa CM, Samanta J, Sherman SJ, et al. Subthalamic nucleus stimulation reverses mediofrontal influence over decision threshold. Nat Neurosci 2011;14:1462–7.
Chiken S, Nambu A. Disrupting neuronal transmission: mechanism of DBS? Front Syst Neurosci 2014;8:33.
Colloca L, Benedetti F, Bergamasco B, Vighetti S, Zibetti M, Ducati A, et al. Electroencephalographic responses to intraoperative subthalamic stimulation. Neuroreport 2006;17:1465–8.
Dalal SS, Zumer JM, Agrawal V, Hild KE, Sekihara K, Nagarajan SS. NUTMEG: a neuromagnetic source reconstruction toolbox. Neurol Clin Neurophysiol 2004;2004:2052.
Delorme A, Makeig S. EEGLAB: an open source toolbox for analysis of single-trial EEG dynamics including independent component analysis. J Neurosci Methods 2004;134:9–21.
Delorme A, Sejnowski T, Makeig S. Enhanced detection of artifacts in EEG data using higher-order statistics and independent component analysis. Neuroimage 2007;34:1443–9.

Delorme A, Mullen T, Kothe C, Akalin Acar Z, Bigdely-Shamlo N, Vankov A, et al. EEGLAB, SIFT, NFT, BCILAB, and ERICA: new tools for advanced EEG processing. Comput Intell Neurosci 2011;130714.

de Hemptinne C, Swann N, Ostrem J, Ryapolova-Webb ES, San Luciano M, Galifianakis NB, et al. Therapeutic deep brain stimulation reduces cortical phase amplitude coupling in Parkinson's disease. Nat Neurosci 2015;18:779–86.

Dostrovsky JO, Lozano AM. Mechanisms of deep brain stimulation. Mov Disord 2002;17(Suppl 3):S63–8.

Dürschmid S, Reichert C, Kuhn J, Freund HJ, Hinrichs H, Heinze HJ. Deep brain stimulation of the nucleus basalis of Meynert attenuates early EEG components associated with defective sensory gating in patients with Alzheimer disease – a two-case study. Eur J Neurosci 2017. https://doi.org/10.1111/ejn.13749 [Epub ahead of print].

Erez Y, Tischler H, Moran A, Bar-Gad I. Generalized framework for stimulus artifact removal. J Neurosci Methods 2010;191:45–59.

Fasano A, Bove F, Lang AE. The treatment of dystonic tremor: a systematic review. J Neurol Neurosurg Psych 2014;85:759–69.

Figee M, Luigjes J, Smolders R, Valencia-Alfonso CE, van Wingen G, de Kwaasteniet B, et al. Deep brain stimulation restores frontostriatal network activity in obsessive-compulsive disorder. Nat Neurosci 2013;16:386–7.

Frysinger RC, Quigg M, Elias WJ. Bipolar deep brain stimulation permits routine EKG, EEG, and polysomnography. Neurology 2006;66:268–70.

Gaggl R. Limitations of delta-sigma converters. In: Delta-sigma A/D-converters, springer series in advanced microelectronics. Heidelberg: Springer Berlin; 2013. p. 15–53.

Gulberti A, Hamel W, Buhmann C, Boelmans K, Zittel S, Gerloff C, et al. Subthalamic deep brain stimulation improves auditory sensory gating deficit in Parkinson's disease. Clin Neurophysiol 2015a;126:565–74.

Gulberti A, Moll CKE, Hamel W, Buhmann C, Koeppen JA, Boelmans K, et al. Predictive timing functions of cortical beta oscillations are impaired in Parkinson's disease and influenced by L-DOPA and deep brain stimulation of the subthalamic nucleus. NeuroImage Clin 2015b;9:436–49.

Hammond C, Ammari R, Bioulac B, Garcia L. Latest view on the mechanism of action of deep brain stimulation. Mov Disord 2008;23:2111–21.

Hescham S, Lim LW, Jahanshahi A, Blokland A, Temel Y. Deep brain stimulation in dementia-related disorders. Neurosci Biobehav Rev 2013;37:2666–75.

Hohlefeld FU, Ehlen F, Krugel LK, Kühn AA, Curio G, Klostermann F, et al. Modulation of cortical neural dynamics during thalamic deep brain stimulation in patients with essential tremor. Neuroreport 2013;24:751–6.

Holiga Š, Mueller K, Möller HE, Urgošík D, Růžička E, Schroeter ML, et al. Resting-state functional magnetic resonance imaging of the subthalamic microlesion and stimulation effects in Parkinson's disease: Indications of a principal role of the brainstem. Neuroimage Clin 2015;9:264–74.

Holtzheimer PE, Mayberg HS. Deep brain stimulation for psychiatric disorders. Annu Rev Neurosci 2011;34:289–307.

Huster RJ, Calhoun VD. Progress in EEG: multi-subject decomposition and other advanced signal processing approaches. Brain Topogr 2018;31:1–2.

Huster RJ, Raud L. A tutorial review on multi-subject decomposition of EEG. Brain Topogr 2018;31:3–16.

Jech R, Urgosik D, Tintera J, Nebuzelsky A, Krasensky J, Liscák R, et al. Functional magnetic resonance imaging during deep brain stimulation: a pilot study in four patients with Parkinson's disease. Mov Disord 2001;16:1126–32.

Jech R, Mueller K, Urgošík D, Sieger T, Holiga Š, Růžička F, et al. The subthalamic microlesion story in Parkinson's disease: electrode insertion-related motor improvement with relative cortico-subcortical hypoactivation in fMRI. PLoS ONE 2012;7:e49056. https://doi.org/10.1371/journal.pone.0049056.

Jech R, Ruzicka E, Urgosik D, Serranova T, Volfova T, Novakova O, et al. Deep brain stimulation of the subthalamic nucleus affects resting EEG and visual evoked potentials in Parkinson's disease. Clin Neurophysiol 2006;117:1017–28.

Kalia SK, Sankar T, Lozano AM. Deep brain stimulation for Parkinson's disease and other movement disorders. Curr Opin Neurol 2013;26:374–80.

Kay SM. Fundamentals of statistical signal processing. Englewood Cliffs, NJ: Prentice-Hall PTR; 1993.

Kibleur A, Polosan M, Favre P, Rudrauf D, Bougerol T, Chabardès S, et al. Stimulation of subgenual cingulate area decreases limbic top-down effect on ventral visual stream: a DBS-EEG pilot study. Neuroimage 2017;146:544–53. https://doi.org/10.1016/j.neuroimage.2016.10.018.

Kim SH, Lim SC, Yang DW, Cho JH, Son BC, Kim J, et al. Thalamo-cortical network underlying deep brain stimulation of centromedian thalamic nuclei in intractable epilepsy: a multimodal imaging analysis. Neuropsychiatr Dis Treat 2017;13:2607–19. https://doi.org/10.2147/NDT.S148617.

Klostermann F, Wahl M, Marzinzik F, Vesper J, Sommer W, Curio G. Speed effects of deep brain stimulation for Parkinson's disease. Mov Disord 2010;25:2762–8.

Ko JH, Tang CC, Eidelberg D. Brain stimulation and functional imaging with fMRI and PET. Handb Clin Neurol 2013;116:77–95.

Kovacs N, Balas I, Kellenyi L, Janszky J, Feldmann A, Llumiguano C, et al. The impact of bilateral subthalamic deep brain stimulation on long-latency event-related potentials. Parkinsonism Relat Disord 2008;14:476–80.

Kringelbach ML, Jenkinson N, Owen SLF, Aziz TZ. Translational principles of deep brain stimulation. Nat Rev Neurosci 2007;8:623–35.

Larson PS. Deep brain stimulation for movement disorders. Neurotherapeutics 2014;11:465–74.

Laxton AW, Lipsman N, Lozano AM. Deep brain stimulation for cognitive disorders. Handb Clin Neurol 2013;116:307–11.

Lempka SF, McIntyre CC. Theoretical analysis of the local field potential in deep brain stimulation applications. PLoS ONE 2013;8:e59839.

Lio G, Boulinguez P. Greater robustness of second order statistics than higher order statistics algorithms to distortions of the mixing matrix in blind source separation of human EEG: implications for single-subject and group analyses. NeuroImage 2013;67C:137–52.

Lio G, Boulinguez P. How does sensor-space group blind source separation face inter-individual neuroanatomical variability? insights from a simulation study based on the PALS-B12 Atlas. Brain Topogr 2018;31:62–75.

Little S, Pogosyan A, Neal S, Zavala B, Zrinzo L, Hariz M, et al. Adaptive deep brain stimulation in advanced Parkinson disease. Ann Neurol 2013;74:449–57.

Lyons MK. Deep brain stimulation: current and future clinical applications. Mayo Clin Procee 2011;86:662–72.

Makeig S, Debener S, Onton J, Delorme A. Mining event-related brain dynamics. Trends Cogn Sci 2004;8:204–10.

Makeig S, Onton J. ERP features and EEG dynamics: an ICA perspective. In: Luck S, Kappenman E, editors. Oxford handbook of event-related potential components; 2009.

MacKinnon CD, Webb RM, Silberstein P, Tisch S, Asselman P, Limousin P, et al. Stimulation through electrodes implanted near the subthalamic nucleus activates projections to motor areas of cerebral cortex in patients with Parkinson's disease. Eur J Neurosci 2005;21:1394–402.

Magrassi L, Maggioni G, Pistarini C, Di Perri C, Bastianello S, Zippo AG, et al. Results of a prospective study (CATS) on the effects of thalamic stimulation in minimally conscious and vegetative state patients. J Neurosurg 2016;125:972–81.

Markser A, Maier F, Lewis CJ, Dembek TA, Pedrosa D, Eggers C, et al. Deep brain stimulation and cognitive decline in Parkinson's disease: the predictive value of electroencephalography. J Neurol 2015;262:2275–84.

McIntyre CC, Savasta M, Kerkerian-Le Goff L, Vitek JL. Uncovering the mechanism(s) of action of deep brain stimulation: activation, inhibition, or both. Clin Neurophysiol 2004;115:1239–48.

Michel C, He B. EEG Mapping and source imaging. In: Schomer D, Lopes da Silva FH, editors. Niedermeyer's Electroencephalography. Philadelphia: Lippincott Williams & Wilkins; 2011. p. 1179–202.

Michel CM, Murray MM. Towards the utilization of EEG as a brain imaging tool. Neuroimage 2012;61:371–85.

Michel CM, Murray MM, Lantz G, Gonzalez S, Spinelli L, Grave de Peralta R. EEG source imaging. Clin Neurophysiol 2004;115:2195–222.

Mideksa KG, Singh A, Hoogenboom N, Hellriegel H, Krause H, Schnitzler A, et al. Comparison of imaging modalities and source-localization algorithms in locating the induced activity during deep brain stimulation of the STN. Conf Proc IEEE Eng Med Biol Soc 2016;2016:105–8. https://doi.org/10.1109/EMBC.2016.7590651.

Miocinovic S, Miller A, Swann NC, Ostrem JL, Starr PA. Chronic deep brain stimulation normalizes scalp EEG activity in isolated dystonia. Clin Neurophysiol 2017;129:368–76. https://doi.org/10.1016/j.clinph.2017.11.011.

Moll CK, Sharott A, Hamel W, Münchau A, Buhmann C, Hidding U, et al. Waking up the brain: a case study of stimulation-induced wakeful unawareness during anaesthesia. Prog Brain Res 2009;177:125–45.

Mückschel M, Smitka M, Hermann A, von der Hagen M, Beste C. Deep brain stimulation in the globus pallidus compensates response inhibition deficits: evidence from pantothenate kinase-associated neurodegeneration. Brain Struct Funct 2016;221:2251–7. https://doi.org/10.1007/s00429-015-1041-8.

Muthuraman M, Paschen S, Hellriegel H, Groppa S, Deuschl G, Raethjen J. Locating the STN-DBS electrodes and resolving their subsequent networks using coherent source analysis on EEG. Conf Proc IEEE Eng Med. Biol Soc 2012:3970–3. https://doi.org/10.1109/EMBC.2012.6346836.

Nyquist H. Certain topics in telegraph transmission theory. Trans AIEE 1928;47:617–44.

Okun MS. Deep-brain stimulation–entering the era of human neural-network modulation. N Engl J Med 2014;371:1369–73.

Onton J, Makeig S. Information-based modeling of event-related brain dynamics. Prog Brain Res 2006;159:99–120.

Oostenveld R, Fries P, Maris E, Schoffelen J-M. FieldTrip: open source software for advanced analysis of MEG, EEG, and invasive electrophysiological data. Comput Intell Neurosci 2011;2011:156869.

Pamarti S. Quantization noise conditioning techniques for digital delta-sigma modulators. In: Proceedings of the 19th international symposium on mathematical theory of networks and systems–MTNS; 2010.

Pascual-Marqui RD. Theory of the EEG inverse problem. In: Tong S, Thakor NV, editors. Quantitative EEG analysis: methods and clinical applications. Boston, MA: Artech House; 2009. p. 121–40.

Phillips MD, Baker KB, Lowe MJ, Tkach JA, Cooper SE, Kopell BH, et al. Parkinson disease: pattern of functional MR imaging activation during deep brain stimulation of subthalamic nucleus–initial experience. Radiology 2006;239:209–16.

Ponce FA, Lozano AM. Deep brain stimulation state of the art and novel stimulation targets. Prog Brain Res 2010;184:311–24.

Priori A, Cinnante C, Genitrini S, Pesenti A, Tortora G, Bencini C, et al. Non-motor effects of deep brain stimulation of the subthalamic nucleus in Parkinson's disease: preliminary physiological results. Neurol Sci 2001;22:85–6.

Quraan MA, Protzner AB, Daskalakis ZJ, Giacobbe P, Tang CW, Kennedy SH, et al. EEG power asymmetry and functional connectivity as a marker of treatment effectiveness in DBS surgery for depression. Neuropsychopharmacology 2014;39:1270–81.

Rezai AR, Phillips M, Baker KB, Sharan AD, Nyenhuis J, Tkach J, et al. Neurostimulation system used for deep brain stimulation (DBS): MR safety issues and implications of failing to follow safety recommendations. Invest Radiol 2004;39:300–3.
Rosa M, Giannicola G, Marceglia S, Fumagalli M, Barbieri S, Priori A. Neurophysiology of deep brain stimulation. Int Rev Neurobiol 2012;107:23–55.
Santillán-Guzmán A, Heute U, Muthuraman M, Stephani U, Galka A. DBS artifact suppression using a time-frequency domain filter. Conf Proc IEEE Eng Med Biol Soc 2013;2013:4815–8.
Selzler K, Burack M, Bender R, Mapstone M. Neurophysiological correlates of motor and working memory performance following subthalamic nucleus stimulation. J Cogn Neurosci 2013;25:37–48.
Shannon CE. Communication in the presence of noise. Proceedings of the Institute of Radio Engineers; 1949;37, p. 10–21.
Scholten M, Govindan RB, Braun C, Bloem BR, Plewnia C, Krüger R, et al. Cortical correlates of susceptibility to upper limb freezing in Parkinson's disease. Clin Neurophysiol 2016a;127:2386–93. https://doi.org/10.1016/j.clinph.2016.01.028.
Scholten M, Klotz R, Plewnia C, Wächter T, Mielke C, Bloem BR, et al. Neuromuscular correlates of subthalamic stimulation and upper limb freezing in Parkinson's disease. Clin Neurophysiol 2016b;127:610–20. https://doi.org/10.1016/j.clinph.2015.02.012.
Siegel M, Donner TH, Engel AK. Spectral fingerprints of large-scale neuronal interactions. Nat Rev Neurosci 2012;13:121–34.
Silberstein P, Pogosyan A, Kühn AA, Hotton G, Tisch S, Kupsch A, et al. Cortico-cortical coupling in Parkinson's disease and its modulation by therapy. Brain 2005;128:1277–91.
Sun L, Hinrichs H. Moving average template subtraction to remove stimulation artifactsin EEGs and LFPs recorded during deep brain stimulation. J Neurosci Methods 2016;266:126–36.
Sun Y, Farzan F, Garcia Dominguez L, Barr MS, Giacobbe P, Lozano AM, et al. A novel method for removal of deep brain stimulation artifact from electroencephalography. J Neurosci Methods 2014;237:33–40.
Sun Y, Giacobbe P, Tang CW, Barr MS, Rajji T, Kennedy SH, et al. Deep brain stimulation modulates gamma oscillations and theta-gamma coupling in treatment resistant depression. Brain Stimulat 2015;8:1033–42.
Swann N, Poizner H, Houser M, Gould S, Greenhouse I, Cai W, et al. Deep brain stimulation of the subthalamic nucleus alters the cortical profile of response inhibition in the beta frequency band: a scalp EEG study in Parkinson's disease. J Neurosci 2011;31:5721–9.
Tadel F, Baillet S, Mosher JC, Pantazis D, Leahy RM. Brainstorm: a user-friendly application for MEG/EEG analysis. Comput Intell Neurosci 2011;2011:879716.
Tang AC, Sutherland MT, McKinney CJ. Validation of SOBI components from high-density EEG. Neuroimage 2005;25:539–53.
Thompson JA, Lanctin D, Ince NF, Abosch A. Clinical implications of local field potentials for understanding and treating movement disorders. Stereotact Funct Neurosurg 2014;92:251–63.
Vidailhet M, Jutras MF, Roze E, Grabli D. Deep brain stimulation for dystonia. Handb Clin Neurol 2013;116:167–87.
Vitek JL. Deep brain stimulation: how does it work? Cleve Clin J Med 2008;75(S2):S59–65.
Wagle Shukla A, Okun MS. Surgical treatment of Parkinson's disease: patients, targets, devices, and approaches. Neurotherapeutics 2014;11:47–59.
Walker HC, Huang H, Gonzalez CL, Bryant JE, Killen J, Knowlton RC, et al. Short latency activation of cortex by clinically effective thalamic brain stimulation for tremor. Mov Disord 2012a;27:1404–12.
Walker HC, Huang H, Gonzalez CL, Bryant JE, Killen J, Cutter GR, et al. Short latency activation of cortex during clinically effective subthalamic deep brain stimulation for Parkinson's disease. Mov Disord 2012b;27:864–73.
Weiss D, Govindan RB, Rilk A, Wächter T, Breit S, Zizlsperger L, et al. Central oscillators in a patient with neuropathic tremor: evidence from intraoperative local field potential recordings. Mov Disord 2011;26(2):323–7.
Weiss D, Breit S, Hoppe J, Hauser AK, Freudenstein D, Krüger R, et al. Subthalamic nucleus stimulation restores the efferent cortical drive to muscle in parallel to functional motor improvement. Eur J Neurosci 2012;35:896–908.
Weiss D, Klotz R, Govindan RB, Scholten M, Naros G, Ramos-Murguialday A, et al. Subthalamic stimulation modulates cortical motor network activity and synchronization in Parkinson's disease. Brain 2015;138:679–93.